AIP Journal of Applied Physics

Acoustic cloaking by extraordinary sound transmission

Jiajun Zhao, Zhi Ning Chen, Baowen Li, and Cheng-Wei Qiu

Citation: Journal of Applied Physics **117**, 214507 (2015); doi: 10.1063/1.4922120
View online: http://dx.doi.org/10.1063/1.4922120
View Table of Contents: http://scitation.aip.org/content/aip/journal/jap/117/21?ver=pdfcov
Published by the AIP Publishing

JOURNAL OF APPLIED PHYSICS **117**, 214507 (2015)

Acoustic cloaking by extraordinary sound transmission

Jiajun Zhao,[1] Zhi Ning Chen,[1] Baowen Li,[2] and Cheng-Wei Qiu[1,a)]
[1]*Department of Electrical and Computer Engineering, National University of Singapore, Singapore 117583, Singapore*
[2]*Department of Physics and Centre for Computational Science and Engineering, National University of Singapore, Singapore 117546, Singapore*

(Received 26 January 2015; accepted 23 May 2015; published online 5 June 2015)

Isotropic acoustic cloaking is proposed using density-near-zero materials for extraordinary sound transmission. The cloaking cell is made by single-piece homogeneous elastic copper, which can be detached and assembled arbitrarily. We theoretically and numerically demonstrate the cloaking performance by deploying density-near-zero cells in various ways in two-dimensional space as well as in acoustic waveguides. The density-near-zero material can make any inside objects imperceptible along undistorted sound paths. Individually and collectively, the cloaking cell maintains both the planar wavefront and the nearly perfect one-dimensional transmission, in presence of any inserted object. The overall cloaked space can be designed by adding cells without the limit of the total cloaked volume. © *2015 AIP Publishing LLC*.
[http://dx.doi.org/10.1063/1.4922120]

I. INTRODUCTION

Various metamaterial-based invisibility cloaking has been demonstrated in optics, acoustics,[1,2] and heat conduction by the theory of transforming coordinates. As a tradeoff, in optics, the spatially tailored properties of metamaterials, usually inhomogeneous and anisotropic, impose challenging complexities in structural configuration and cloaking realization.[3,4] As the acoustic analog of transformation optics,[5] the experimental realization of acoustic cloaking was reported,[6,7] but its inhomogeneous acoustic inertia and modulus caused by coordinate transformation inevitably result in the same challenges as in optics. More recently, a topological-optimization method was invented to cancel acoustic scattering by wave interference,[8,9] which only requires a specific optimized distribution of rigid boundaries around the object to be hidden. Although this scheme does not require considering a complex structure of artificial metamaterials, topological acoustic cloaking highly relies on the shape and the locus of the object to be hidden. Therefore, the object actually is a part of the cloaking device itself. It implies that the cloaking structure designed for one object has to be redesigned for another, which has different shapes, locus, or material composition.

Therefore, to construct an isotropic acoustic cloaking, independent of the cloaked objects in two-dimensional (2D) space or in curved waveguides, could be meaningful in both theory and application. Here, we propose a cloaking structure, which sustains the characteristics of the reported acoustic cloaks derived by transformation acoustics, and which is also able to overcome the defect of topologically optimized cloaks. Our acoustic cloaking cell is only made of single-piece homogeneous elastic copper in an accessible structure, including one pressure absorber and one pressure projector connected by an isolated energy channel. The elastic material can be regarded at a certain frequency as an effective density-near-zero (DNZ) material. Due to the mechanical resonance of the elastic structure, the phase velocity of sound waves in the cloaking setup almost reaches infinite value and consequently, extraordinary sound transmission (EST) is expected.[10,11] The cloaking performance by our structure is explained by simplified theoretical model and verified by numerical simulation in 2D space as well as curved waveguides.

[a)]Author to whom correspondence should be addressed. Electronic mail: eleqc@nus.edu.sg

II. CLOAKING CELL MADE BY HOMOGENEOUS AND ISOTROPIC MATERIAL

To illustrate the concept of our design, we compare it with acoustic cloaking based on coordinate transformation[12] in Fig. 1(a), which renders an object invisible by distorting its ambient flow. The scheme of the proposed DNZ acoustic-cloaking cell in Fig. 1(b) can produce EST to hide arbitrary inserted objects as well as to preserve wavefronts and phases.

Conceptually, the flow at the front of an object is concentrated into the energy channel by an absorber. Then, acoustic energy is coupled out by a projector to the back side where the flow is restored. The entire process resembles the engineering optical camouflage: positioning cameras upon an object wrapped by a retro-reflecting coat; taking pictures and transmitting the signal; and projecting the front scene onto the back of the coat.[13] In Fig. 1(b), acoustic cloaking for one-dimensional (1D) invisibility can be achieved without wave distortion along sound paths, and the length of the cloaking device is designed to maintain the phase continuity at both sound inlet and outlet. Additionally, our design is completely irrelevant to the positions, quantities, or the shapes of the inside hidden objects, distinct from the way of topological-optimization method.[9]

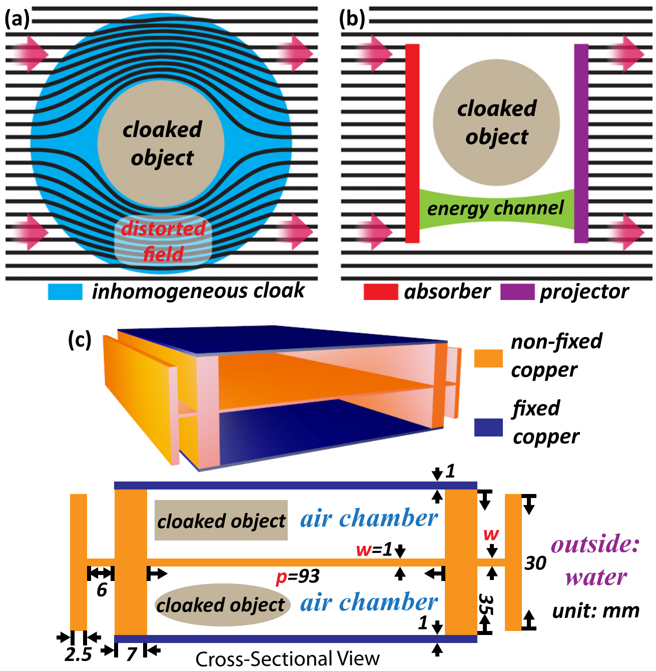

FIG. 1. Comparison of (a) traditional acoustic cloaking based on coordinate transformation and (b) our cloaking by a density-near-zero cell for extraordinary sound transmission. (c) Our cell consists of one single-piece copper with air chambers inside it, and it is immersed in water.

The DNZ acoustic-cloaking cell shown in Fig. 1(c) is only implemented by copper (density: 8900 kg/m^3; Young's modulus: 122 GPa; Poisson's ratio: 0.35)[14] with two fixed planks (blue parts). p and w are the length and width of the energy channel, respectively. The two hollow enclosed chambers are designed to fill with air (density: 1.21 kg/m^3; speed of sound: 343 m/s), where any objects can be placed inside for the purpose of invisibility. The T-shaped protrusion at each end is used as the locally resonant element to enhance sound transmission.[15,16] The entire structure is immersed in water (density: 998 kg/m^3; speed of sound: 1481 m/s), and a monochromatic acoustic plane wave propagates from left to right. The COMSOL software has been used to do simulation.

The acoustic power transmission through the DNZ acoustic-cloaking cell immersed in water is numerically simulated. In Fig. 2(a), there are two frequencies that allow EST (13.45 kHz and 23.1 kHz) with a small peak (16.3 kHz) in between. We also calculate the vibration states at the three frequencies in Figs. 2(b)–2(d). Figs. 2(b) and 2(c) show by simulation two opposite resonances of the DNZ cell. Inside the cloaking cell, the internal motion is simply the longitudinal movement of the elastic energy channel, which can be seen at displacement fields. We furthermore individually calculate the eigenfrequencies of the copper parts, shown as the purple dots in Fig. 2(a). The similarity between the frequencies that correspond to the red dots and that correspond to the purple dots shows that by the systematic resonance the structured cell is capable of total power transmission, as the requirement of acoustic cloaking. The slight disagreement between the dots of different colors is because that for the red dots that correspond to Figs. 2(b) and 2(c), the acoustic load from the ambient water has been taken into account,

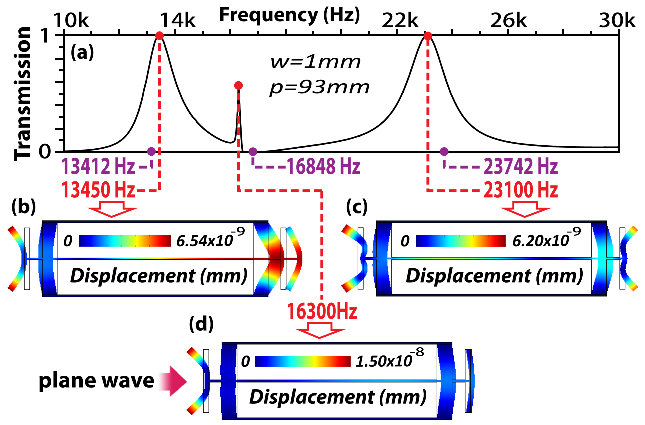

FIG. 2. Simulated sound transmission through the density-near-zero cell. The transmission shown in (a) is a function of the frequency of the normally-incident sound waves. The three purple dots indicate the eigenfrequencies of the copper part, and the three red dots indicate the frequencies at the three peaks. The displacement of the structure at input frequencies (three peaks) is shown in (b)–(d), respectively.

while for the purple dots, we only consider the eigenfrequencies of the copper parts.

III. SPRING-MASS MODEL AND DENSITY-NEAR-ZERO PROPERTY

Our design focuses on achieving the DNZ property by using the structural resonance, and meanwhile isolating the objects to be hidden from the entire resonance system. A spring-mass model, the mechanical translation of acoustic systems,[17] is illustrated here to expound the resonance and the consequent DNZ property.

The cell immersed in water in Fig. 3(a) can be regarded as the damping spring-mass model in Fig. 3(b). In Fig. 3(a), different parts of the cell are tinted with different colors to illustrate the counterpart elements in Fig. 3(b). Specifically, we regard the fixed copper planks (black) as the fixed wall (black), the input sound as the driving force (pink), and the

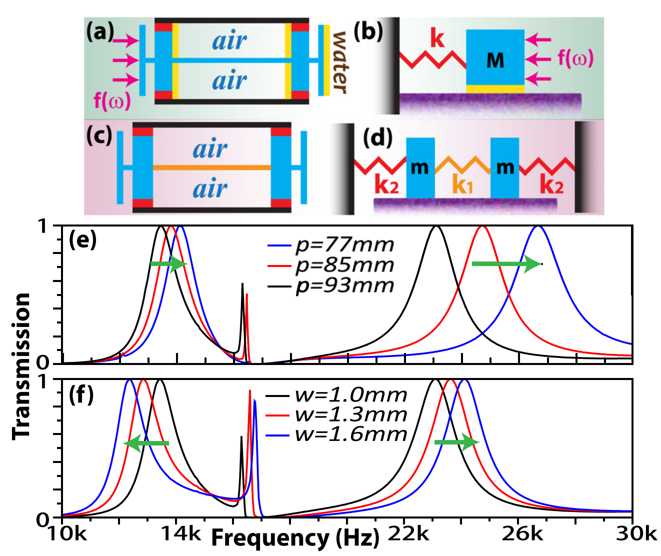

FIG. 3. (a) and (c) Schematics of the acoustic-cloaking cell. Different colors stand for different parts of the cell. (b) The spring-mass model. (d) The coupling model. (e) and (f) The power transmission as a function of the input sound frequency when the shape of the energy channel is changed.

main body of the cell as the mass chunk (blue). The joints (red) as well as the elasticity of the cell are rationally modeled as the ideal spring (red). The acoustic impedance exerted upon boundaries (yellow) is modeled as frictional damping, because when the cell vibrates, it will fight against the resistance from the outside water and the inside air. Therefore, the equation for this spring-mass model becomes

$$Md^2x/dt^2 = -kx - \gamma M dx/dt + F_0 \cos \omega t, \tag{1}$$

where k denotes the stiffness of the ideal spring in Fig. 3(b); γ is the damping coefficient; M is the mass of the chunk; x is the displacement; ω is the driving frequency; and $F_0 \cos \omega t$ is the driving force. The resonant frequency in the case of no damping is $\omega_0 = \sqrt{k/M}$. Then, the solution of Eq. (1) becomes $x = A\cos(\omega t - \delta)$, where $A = F_0/[M\sqrt{({\omega_0}^2 - \omega^2)^2 + (\omega\gamma)^2}]$ and $\tan\delta = \omega\gamma/({\omega_0}^2 - \omega^2)$. The maximum amplitude occurs at $\omega_1 = \sqrt{{\omega_0}^2 - \gamma^2/2}$. If there is no friction $\gamma = 0$, the driving frequency is ω_0 and A goes up infinitely, and the mechanical energy of the vibrating chunk is accumulated because of the driving force. However, if there is a damping effect, e.g., the friction between the ground and the chunk, the accumulated energy at the resonance will be conveyed to dissipation, making the system in its steady state. Under this circumstance, A will remain a finite maximum when $\omega = \omega_1$.

Due to energy conservation, all input power will be consumed by the friction, and the driving energy is transferred wherever the damping (yellow) is. As the comparison in Fig. 3(a), the force from the input wave not only drives the vibration of the DNZ cell but also needs to overcome the resistances at the solid-liquid interfaces (yellow). Therefore, at systematic resonances, the momentum gain of the acoustic loads, i.e., the inside air and the outside water, consumes all the cumulative input acoustic power. Consequently, at the moment of systematic resonances, the entire system is in its steady state.

Moreover, since the acoustic impedance of the outside water is extremely higher than that of the inside air (3561 times), the acoustic load is almost completely attributed by water. Thus, all input power is expected to be transferred to outside water, which leads to EST. By this way, the objects to be hidden inside the cloaked space are isolated from the systematic resonance of the DNZ cell, because the air chambers decouple the systematic resonance from the existence of the inside objects. The decoupling effect is not considered by the traditional design of membrane-induced DNZ metamaterials.[11]

Instead of the major resonances, there are several other minor resonances due to the rich oscillation modes of solids, which are not observable simply based on simplified 1D spring-mass model. However, the spring-mass model is the classic approach to explain the underlying mechanism of EST and the cause of the acoustic cloaking effect in our design.

Additionally, the spring-mass model implies the DNZ property of the cell at its resonance, which is the acoustic equivalent of an electromagnetic epsilon-near-zero metamaterial.[19] We may define the effective mass of the vibration system as $M_{eff}(\omega) = M - k/\omega^2$, which intrinsically includes the acoustic inertance caused by its mass as well as the acoustic compliance caused by its elasticity. The combination of the acoustic compliance and the inertance is the exact analog of the combination of spring compliance and substantial mass in a spring-mass model.

Since the restoring force from the elastic copper of our structure is able to add a negative term to the effective mass, we can rearrange Eq. (1) considering the harmonic vibration[10]

$$F_0 \cos \omega t - \gamma M dx/dt = M_{eff}(\omega) d^2x/dt^2, \tag{2}$$

which turns into the form of Newton's second law: driving force – resistance = mass $\times d^2x/dt^2$. At systematic resonance, $M_{eff}(\omega) = M - k/\omega^2$ becomes zero, so that power transmission of input sound is expected to be extremely enhanced.[10] The causality from the DNZ property of our structure to the resultant EST was elaborated in Ref. 10, where a similar membrane-mass model was proposed. (The detailed derivation of the transmission coefficient was given in the Ref. 10 using the lumped element approach.) Actually, the DNZ effect is an innate property of a *dynamic* structure with a certain eigen-vibration excited. For our proposed structure, the DNZ cell at resonance is explained by the aid of the damping spring-mass model in Figs. 2(a) and 2(b).

However, it is noteworthy that although the dynamic density of the individual cell is near zero, the acoustic impedance of the entire acoustic cloaking setup is not near zero at all. When the system vibrates, there will be additional radiation impedance exerted at both ends of the cell. When the systematic resonances occur, EST surely implies the impedance match between the proposed structure and the surrounding. The impedance match in such case is dominantly attributed by the radiation impedance, apart from the minor contribution from the DNZ structure itself. Thus, if taken into account the radiation impedance, the overall acoustic impedance is no more near zero.

IV. COUPLING MODEL AND GEOMETRICAL DEPENDENCE

After discussing the mechanism of the DNZ acoustic-cloaking cell, we further examine the geometrical dependence of the power transmission spectrum, by employing the coupling model in Figs. 3(c) and 3(d).

Analogously to the discussion in terms of Figs. 3(a) and 3(b), the fixed copper planks in Fig. 3(c) (black) can be modeled as the two hard walls (black) in Fig. 3(d). To investigate the dependence between the structural geometry and the resonance, the main bodies in Fig. 3(c) are modeled separately. In this way, the two copper bodies (blue) are modeled as the two chunks (blue) with mass m. The four joints (red) indicating elasticity are interpreted as the two ideal springs (red) with stiffness k_2, connecting the chunks to the walls. Additionally, owing to the narrowness of the energy channel (orange), we model it as the spring with stiffness k_1 and mass m_s (orange), which couples the two chunks. By the coupling model, we discover the dependence between the

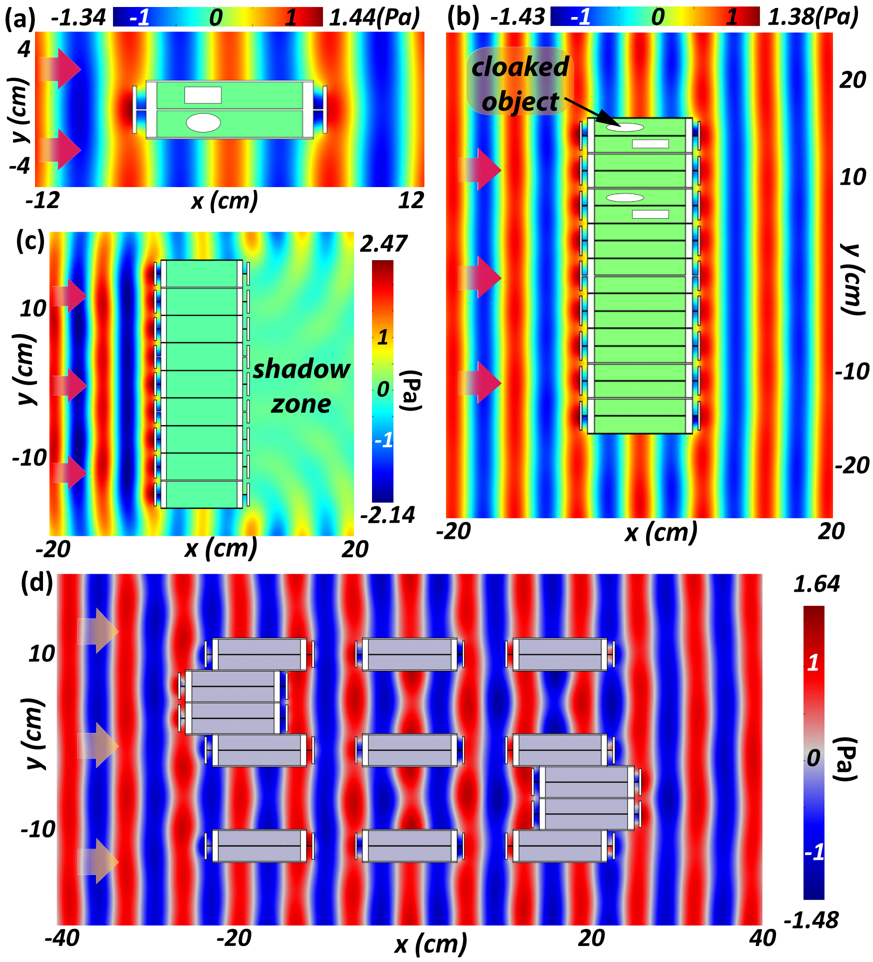

FIG. 4. Applying the cells for acoustic cloaking in unbounded space filled with water. (a) Two objects are hidden inside the cell. There is no sound inside air chambers, and the field outside the cell is almost unperturbed. (b) The density-near-zero array is immersed in water, and the wavefront and the phase are restored at its back. (c) When the energy channels are removed, strong scattering occurs. (d) Multiple cells form an S-shaped cloaked space.

structural geometry of the DNZ cell and the working frequencies of EST.

The equations for the coupling model shown in Figs. 3(c) and 3(d) are

$$\begin{cases} md^2x_1/dt^2 = -k_2x_1 + k_1(x_2 - x_1) - \gamma m dx_1/dt, \\ md^2x_2/dt^2 = -k_1(x_2 - x_1) - k_2x_2 - \gamma m dx_2/dt, \end{cases} \tag{3}$$

where x_1 and x_2 are the displacements of the left and the right chunks. The lower and higher resonant frequencies of Eq. (3) are $\omega_L = \sqrt{k_2/(m+m_s) - \gamma^2/4}$ and $\omega_H = \sqrt{(2k_1+k_2)/(m+m_s) - \gamma^2/4}$, respectively. If the energy-channel length $p = 93$ mm in Fig. 1(c) becomes longer, m_s will become larger but k_1 will get smaller, similarly to the serial connection of springs. Therefore, both ω_L and ω_H will become smaller, which implies that all resonant frequencies of the DNZ cell will be shifted lower when p becomes longer. Vice versa, if the energy-channel length is shortened the resonant frequencies will be shifted higher. The shift observed from the curves in Fig. 3(e) validates the theoretical spring-model analysis.

If the channel width $w = 1.0$ mm becomes thicker, m_s as well as k_1 will become larger, similarly to the shunt connection of springs. Therefore, ω_L will become even lower. As for ω_H, the double increments of k_1 at the numerator $(2k_1 + k_2)$ is empirically larger than the increment of m_s at the denominator, leading to the rise of ω_H. Thus, we can predict that if w gets thicker, the low resonant frequencies of the DNZ cell will be shifted even lower, whereas the high resonant frequencies will be even higher. The broadening of the power transmission spectrum in Fig. 3(f) verifies our analysis.

We investigate the geometrical dependence in terms of the sound-tunneling channel inside the cloaking cell, which is the key component of our structure. However, the two terminal chunks of the cloaking cell cannot be straightforwardly characterized by spring-mass model. The solid eigenvibration of the chunks is 2D, which is hard to be interpreted by 1D model. The precise analysis of the solid chunks needs direct numerical simulation.

V. DEPLOYING CLOAKED AREA

We numerically examine the acoustic pressure field distribution in the domain where the proposed DNZ cell is immersed in water, while the monochromatic acoustic waves are normally incident from left with unit magnitude and frequency 23.1 kHz. As expected, inside the air chambers in Fig. 4(a), there is no sound penetration, which means the inserted objects are isolated and decoupled to the systematic resonance and the outside field. It is remarkable that the power transmission nearly reaches 100%, which implies EST through the DNZ cell with no backscattering.

Also, we notice in Fig. 4(a) that the phase at the inner side of the T-shaped ends is not continuous because of the

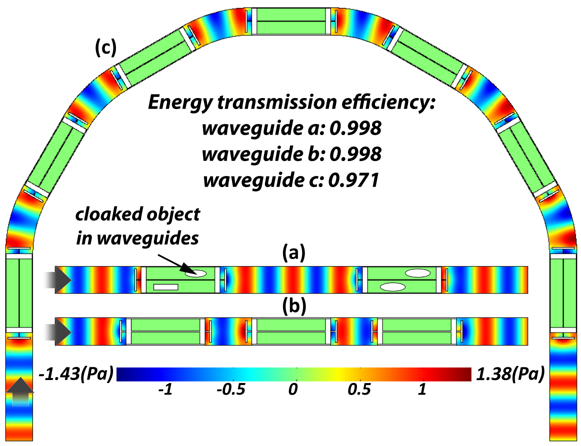

FIG. 5. Applying the cells for acoustic cloaking in waveguides. (a) Four objects in a straight waveguide are hidden inside the cells. There is no sound inside air chambers, and the outside traveling sound is largely transmitted. (b) The number of cells does not affect the resonant frequencies. (c) The high power transmission shows that the cells are able to hide inside objects as well as to bend sound in waveguides.

perturbation from the local resonances inside the concaves of the T-shaped ends. However, the phase at the outer side of the T-shaped ends is almost the same as the adjacent ambient phase. The length of the cell is also designed to maintain the phase continuity at the sound outlet, which makes the plane wavefront instead of other curved wavefront propagate out.

Furthermore, thanks to the rigid boundaries at the two fixed planks in Fig. 1(c), we can connect as many cells sharing the planks as possible, to form an arbitrarily designed cloaked space. In Fig. 4(b), the cells are aligned side by side to increase the acoustic-cloaking volume. The cloaking effect is demonstrated that the bulky copper array itself and the multiple objects inside the cell are imperceptible from outside. Contrarily, if the energy channels are removed, strong backscattering will occur as shown in Fig. 4(c). We can also design the overall cloaked space with an arbitrary distribution of the cells [see Fig. 4(d) where an S-shaped cloaked space is formed]. Based on the proposed detachable DNZ cells, we accomplish arbitrary acoustic cloaking in 2D space only by a single kind of uniform isotropic material.

Besides the scenario in 2D space, sound manipulation in waveguides showed significant applications as well, such as the acoustic circulator based on non-reciprocity.[18] Here, the DNZ cell is also functional in cloaking objects in waveguides. As shown in Fig. 5(a), where acoustic waves propagate through the hard-wall waveguide filled with water, the objects inside the air chambers are imperceptible. Note that one characteristic of DNZ property is that energy tunneling occurs independently of the number of DNZ segments, because each DNZ segment is able to resonate at the same frequency without influencing each other.[11] Even if we add more cells inside the waveguide, the resonant frequency will not be shifted, as shown in Fig. 5(b). The energy transmission is almost 100% in both Figs. 5(a) and 5(b), which indicates EST happens through DNZ cells. In Fig. 5(c), we further demonstrate the acoustic cloaking effect along a curved waveguide, which is used to bend sound path and to maintain the cloaking effect simultaneously as designed.

VI. CONCLUSION

We design an acoustic-cloaking cell that has the density-near-zero property and is able to eliminate the perceptibility of inside objects from underwater sound. The design is inspired by the combination of acoustic inertance and acoustic compliance of the structure at systematic resonances. A plane wavefront is maintained without distortion, and the reflection is dramatically suppressed due to extraordinary sound transmission. Note that the density-near-zero cell for acoustic cloaking is built only by a uniform material, while its cloaking effect is independent of the objects inside it. Moreover, such density-near-zero cells are detachable, and therefore robust in being assembled to change or expand the overall cloaked space with no limit in volume and distribution. The flexibility can be universally applied in unbounded space as well as in waveguides. We believe the proposed density-near-zero cell may open a distinct and concise way to acoustic cloaking by using natural bulky materials.

[1]N. H. Gokhale, J. L. Cipolla, and A. N. Norris, J. Acoust. Soc. Am. **132**, 2932 (2012).
[2]A. N. Norris and A. L. Shuvalov, Wave Motion **48**, 525 (2011).
[3]D. Schurig, J. J. Mock, B. J. Justice, and S. A. Cummer *et al.*, Science **314**, 977 (2006).
[4]N. H. Gokhale, J. L. Cipolla, and A. N. Norris, J. Acoust. Soc. Am. **132**, 2932 (2012).
[5]A. N. Norris, Proc. R. Soc. A **464**, 2411 (2008).
[6]S. Zhang, C. Xia, and N. Fang, Phys. Rev. Lett. **106**, 024301 (2011).
[7]B. I. Popa, L. Zigoneanu, and S. A. Cummer, Phys. Rev. Lett. **106**, 253901 (2011).
[8]V. M. García-Chocano, L. Sanchis, A. Díaz-Rubio, J. Martínez-Pastor *et al.*, Appl. Phys. Lett. **99**, 074102 (2011).
[9]L. Sanchis, V. M. García-Chocano, R. Llopis-Pontiveros, A. Climente *et al.*, Phys. Rev. Lett. **110**, 124301 (2013).
[10]J. J. Park, K. J. B. Lee, O. B. Wright, M. K. Jung *et al.*, Phys. Rev. Lett. **110**, 244302 (2013).
[11]R. Fleury and A. Alù, Phys. Rev. Lett. **111**, 055501 (2013).
[12]*Acoustic Metamaterials*, edited by R. V. Craster and S. Guenneau (Springer, 2013).
[13]S. Tachi, "Telexistence and retro-reflective projection technology," in Proceedings of the 5th Virtual Reality International Conference, Laval Virtual, France, 13–18 May 2003.
[14]D. T. Blackstock, *Fundamentals of Physical Acoustics* (Wiley, New York, 2000).
[15]Z. Liu, X. Zhang, Y. Mao, Y. Y. Zhu, Z. Yang, C. T. Chan, and P. Sheng, Science **289**, 1734 (2000).
[16]Y. Li, B. Liang, X. Y. Zou, and J. C. Cheng, Chin. Phys. Lett. **29**, 114301 (2012).
[17]L. E. Kinsler, A. U. Frey, A. B. Coppens, and J. V. Sanders, *Fundamental of Acoustics* (Wiley, New York, 1982).
[18]R. Fleury, D. L. Sounas, C. F. Sieck, M. R. Haberman, and A. Alù, Science **343**, 516 (2014).
[19]Z. Yang, J. Mei, M. Yang, N. H. Chan, and P. Sheng, Phys. Rev. Lett. **101**, 204301 (2008).